Nanoscale

Impact of nanopillars on phonon dispersion and thermal conductivity of silicon membranes

Journal:	*Nanoscale*
Manuscript ID	NR-ART-11-2022-006266.R1
Article Type:	Paper
Date Submitted by the Author:	15-Dec-2022
Complete List of Authors:	Anufriev, Roman; The University of Tokyo, IIS Ohori, Daisuke; Tohoku University Institute of Fluid Science, Innovative Energy Research Center Wu, Yunhui; The University of Tokyo, IIS Yanagisawa, Ryoto; The University of Tokyo, IIS Jalabert, Laurent; University of Tokyo, Samukawa, Seiji; Tohoku University, Institute of Fluid Science; Tohoku University, WPI Advanced Institute for Materials Research Nomura, M.; The University of Tokyo, IIS

Journal Name

ARTICLE TYPE

Cite this: DOI: 00.0000/xxxxxxxxxx

Impact of nanopillars on phonon dispersion and thermal conductivity of silicon membranes

Roman Anufriev,*[a] Daisuke Ohori,[b], Yunhui Wu,[a], Ryoto Yanagisawa,[a], Laurent Jalabert,[a,c], Seiji Samukawa,[e,f,b,d] and Masahiro Nomura[a]

Received Date
Accepted Date

DOI: 00.0000/xxxxxxxxxx

The performance of silicon-based thermoelectric energy generators is limited by the high thermal conductivity of silicon. Theoretical works have long proposed reducing the thermal conductivity by resonant phonon modes in nanopillars placed on the surface of silicon films. However, these predictions have never been confirmed due to the difficulty in the nanofabrication and measurements of such nanoscale systems. In this work, we report on the fabrication and measurements of silicon films with nanopillars as small as 12 nm in diameter. Our Brillouin light scattering spectroscopy experiments revealed that nanopillars indeed host resonant phonon modes. Yet, our thermal measurements using the micro time-domain thermoreflectance technique showed only a statistically insignificant difference between the thermal properties of silicon membranes with and without nanopillars. Results of this work contrast with the predictions of a substantial reduction in the thermal conductivity due to nanopillars and suggest refining the simulations to account for realistic experimental conditions.

Introduction

Thermoelectrics is a promising technology for green energy harvesting[1,2] Yet, despite the advantages of silicon as a green thermoelectric material, its high thermal conductivity hinders the performance of silicon-based thermoelectric generators[3]. Over the past decade, various methods have been proposed to reduce the thermal conductivity of silicon[4–8] Among them, methods of surface nano-structuring seem particularly promising as they offer to reduce the thermal conductivity while preserving the high electrical conductivity of the material[9–12]. One of such methods suggests fabrication of nanopillars on the surface of silicon films[13].

The nanopillars can change phonon dispersion of the underlying material via two distinct mechanisms: a Bragg interference caused by periodicity of the pillars and local resonances inside the pillars regardless of their periodicity[14,15]. Both of these mechanisms can cause flattening of the dispersion branches of underlying material, which is associated with lower phonon group velocity and reduced thermal conductivity[16,17]. Moreover, the nanopillars can cause additional incoherent phonon scattering, which also reduces the thermal conductivity[18–20].

However, the experimental attempts to demonstrate these effects remain inconclusive[21]. On the one hand, measurements of the phonon dispersion detected resonant pillar modes only at frequencies around several gigahertz[22–26], which is negligibly low as compared to the terahertz-wide spectrum of thermal phonons. On the other hand, thermal measurements could not conclusively link localization in pillars with the reduction in thermal conductivity. Some experiments detected the reduced thermal conductivity but attributed it to diffuse surface scattering of phonons induced by the pillars[27,28]. Recent experiments with more promising nanopillars could not detect any reduction in the thermal conductivity at all[29]. Yet, these experimental attempts could have been hindered by the large size of the pillars or their limited height compared to their diameter and thickness of the underlying membrane. Indeed, theoretical studies typically simulate nanopillars of a few nanometers in size and suggest that taller nanopillars should make a stronger impact on the thermal conductivity[19,30].

In this work, we investigate the impact of local resonances in nanopillars of 12 nm in diameter and 50 nm in height on the phonon and thermal transport in 50-nm-thick silicon membranes. Our acoustic and thermal experiments probe the impact of these pillars on the phonon dispersion and thermal conductivity of silicon membranes. We discuss the implications of the experimental results and suggest the directions of future research.

[a] Institute of Industrial Science, The University of Tokyo, Tokyo 153-8505, Japan; E-mail: anufriev@iis.u-tokyo.ac.jp
[b] Institute of Fluid Science, Tohoku University, Sendai, 980-8577, Japan.
[c] Laboratory for Integrated Micro Mechatronic Systems/National Center for Scientific Research-Institute of Industrial Science (LIMMS/CNRS-IIS), The University of Tokyo, Tokyo 153-8505, Japan.
[d] Advanced Institute for Materials Research, Tohoku University, Sendai, 980-8577, Japan.
[e] Department of Electrical and Computer Engineering, National Yang Ming Chiao Tung University, Hsinchu, Taiwan 300.
[f] Joint Research Center of National Yang Ming Chiao Tung University and Tohoku University, National Yang Ming Chiao Tung University, Hsinchu, Taiwan 300.

Fabrication of nanopillars

The samples were fabricated on a silicon-on-insulator wafer with a 100-nm-thick top silicon layer. First, a SiO_2 film of a few nanometers was synthesized using neutral beam oxidation. Next, ferritin molecules have been uniformly deposited by spin-coating polyethylene-glycol-modified (10 000 molecular weight) ferritin solution on the surface, as shown in Fig. 1a. After removing a protein shell from the ferritin molecules by annealing, the oxide between the cores has been removed using the H_2 radical treatment. Then, half of the top silicon layer was etched using pure chlorine neutral beam with the iron cores serving as a mask. On a reference wafer, no ferritin molecules were deposited, and hence a pristine 50-nm-thick silicon layer was formed. More details on the fabrication process can be found in our previous reports[31,32].

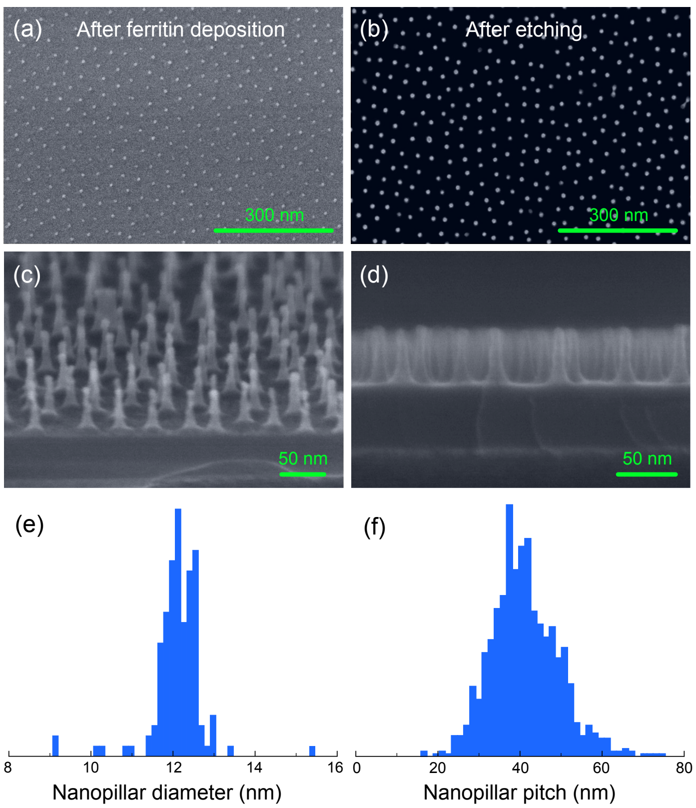

Fig. 1 Scanning electron microscopy images of the wafer (a) after the ferritin mocules deposition and (b-d) after the etching. Distribution of nanopillar (e) diameters and (b) pitch.

Figure 1b-d shows the resulting nanopillars. The nanopillars have a diameter of 12 nm (Fig. 1e), a height of 50 nm, and are evenly distributed on the surface with a distance between nanopillars of 40 $\pm$ 10 nm (Fig. 1f). Although these nanopillars are still larger than atomic scale nanopillars studied in most simulations[13,30,33], these dimensions are close to the design proposed by Davis and Hussein[13] and only about twice larger that those studied by Honarvar et al.[33].

Phonon dispersion measurements

The nanopillars are expected to impact the thermal transport via the phonon resonances that occur in the nanopillars and create flat bands in the phonon dispersion[13]. To detect if such resonant states occur in our nanopillars, we measured the phonon dispersion in our samples using the Brillouin-Mandelstam light-scattering (BLS) spectroscopy[34].

Figure 2a illustrates the BLS method, in which an incident laser beam (λ = 532 nm) is focused on the sample surface at an angle θ, which can be changed to probe a different wavevectors, related to the angle as $q = 4\pi \sin(\theta)/\lambda$. To obtain the phonon spectrum at a given wavevector, a tandem Fabri-Perot interferometer analyses the spectral shift of the inelastically scattered light from the frequency of the incident laser. The interferometer enables measurements of the spectrum with a fine resolution of less than 0.2 GHz.

First, to verify that our BLS setup is able to measure phonon modes in the frequency range of interest and with a required resolution in wavevector, we measured the phonon dispersion of a reference 200-nm-thick suspended silicon membrane. The membrane serves as a calibration sample with a well-known phonon dispersion often measured with the BLS technique[22,35]. Figure 2b shows the measured phonon dispersion with three phonon modes: two fundamental symmetric and antisymmetric modes and one higher symmetric mode. The frequency of the modes is consistent with the predictions of the finite element method (FEM) simulations, performed using material parameters proposed by Graczykowski et al.[22].

Next, we measured samples with and without nanopillars on the surface. The reference wafer without the nanopillars shows only bulk modes of the buried oxide layer under the silicon layer (Fig. 2c), albeit 2 GHz lower than predicted by FEM simulations. For the wafer with the nanopillars (Fig. 2d), simulations predicted resonant modes around 5 GHz, 26 GHz and higher frequencies. Our BLS spectroscopy experiment detected only the first mode around 5 GHz. The flat shape of the 5 GHz mode implies zero group velocity of phonons at this state, suggesting that this is the mode likely localized inside the nanopillars. However, the modes at higher frequencies remained invisible, which is consistent with BLS measurements reported in the literature, where the localized pillar modes are typically observed at frequencies not exceeding several gigahertz[22–26].

Figure 2e show eigenfrequencies in our silicon nanopillars predicted by FEM simulations. The spectrum consists of hundreds of modes below 1 THz and only becomes denser at higher frequencies. Theoretical works suggest that the thermal conductivity reduction is proportional to the density of localized modes in the phonon spectrum[13,19], and that even several modes can substantially reduce the thermal conductivity[36]. Our nanopillars and their eigenmodes are close to those originally studied by Davis and Hussein (80-nm-tall pillars of 20 nm in diameter on 50-nm-thick membrane)[13]. Thus, we can expect up to the predicted 40% reduction in the thermal conductivity[13] if some of these resonant modes are thermally excited and coupled to the modes of the underlying membrane.

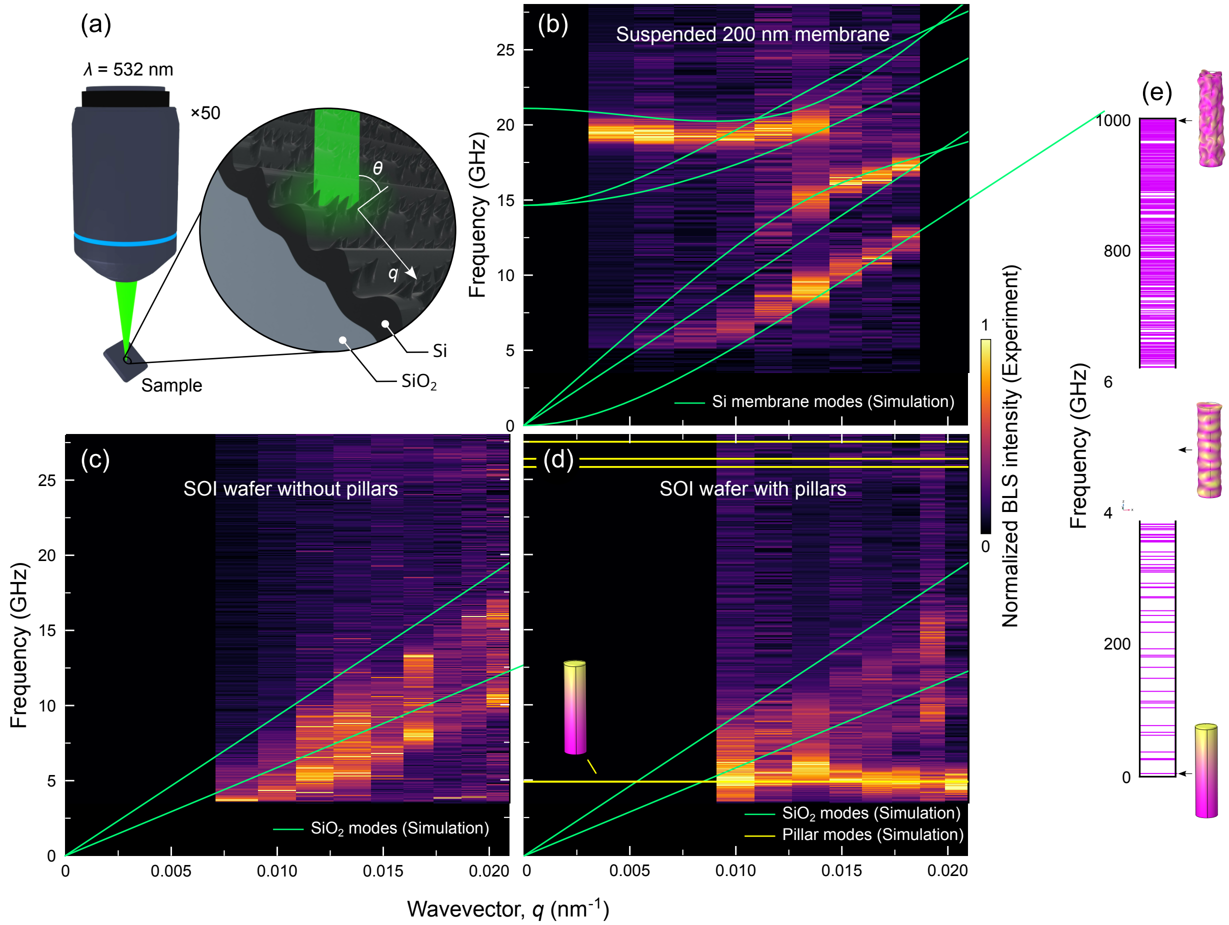

Fig. 2 (a) Scheme of the BLS experiment. (b) Measured phonon dispersion of a reference 200-nm-thick silicon membrane. Measured phonon dispersions of silicon-on-insulator wafers (c) without and (d) with nanopillars on the surface. Color maps show the experimental data obtained using BLS spectroscopy and solid lines show the predictions of FEM simulations for (b) suspended silicon membrane, (c) SiO_2 layer, and (d) a single nanopillar. (e) Eigenfreqencies of silicon nanopillars obtained with FEM simulations.

Thermal conductivity measurements

Next, we investigated how the thermal properties are affected by the presence of nanopillars and their resonant modes. To measure the thermal properties, we used the micro time-domain thermoreflectance (μTDTR) method. This experimental method has previously been used to measure the impact of surface roughness and amorphization on thermal conductivity of silicon nanostructures[9,27,37], and thus is proven to be sensitive to the expected change of 40%. In this photothermal method (Fig 3a), a gold pad in the center of the structure is periodically heated by the pulses of the pump laser (490 nm). The energy absorbed by the pad from each pump pulse can be dissipated only through the three membranes supporting the island with the pad. Thus, by studying the gradual cooling of the pad, we can gain insight into the thermal properties of the membranes. The gradual cooling of the pad is observed using a continuous-wave probe laser (514 nm). This gradual cooling with time t can be well fitted by an exponential function $\exp(-t/\tau)$. The decay time constant τ describes the time of heat dissipation through the membranes connecting the gold pad to the heat sink. The experiments were performed in a closed-cycle helium cryostat, which enables measurements of the thermal properties in a vacuum at different temperatures.

For these measurements, we deposited four gold pads on each wafer and formed three one-micron-wide bridges around each gold using electron-beam lithography and reactive ion etching. Then, the structures were suspended by vapor etching of the buried oxide layer. Unfortunately, the vapor etching process inevitably affects the nanopillars making them thinner and shorter as the oxide layer is repeatedly etched away from the pillars. Despite our best efforts and various fabrication strategies, some degree of pillar degradation appeared unavoidable when nanopillars are exposed to acids or plasma. Figure 3b shows a resulting structure for the μTDTR experiment. More details on the fabrication process and the measurement technique can be found in our previous works[38,39].

First, we measured the thermal decay times τ for four samples on each wafer in the 4 – 300 K range. Figure 3c shows examples of measured decay curves and a Gaussian distribution of 100 decay times τ measured on one sample. Averaged over four samples, Figure 3d shows that the decay times of the membranes with and without nanopillars are the same within the standard deviation in these four measurements. Even at low temperatures,

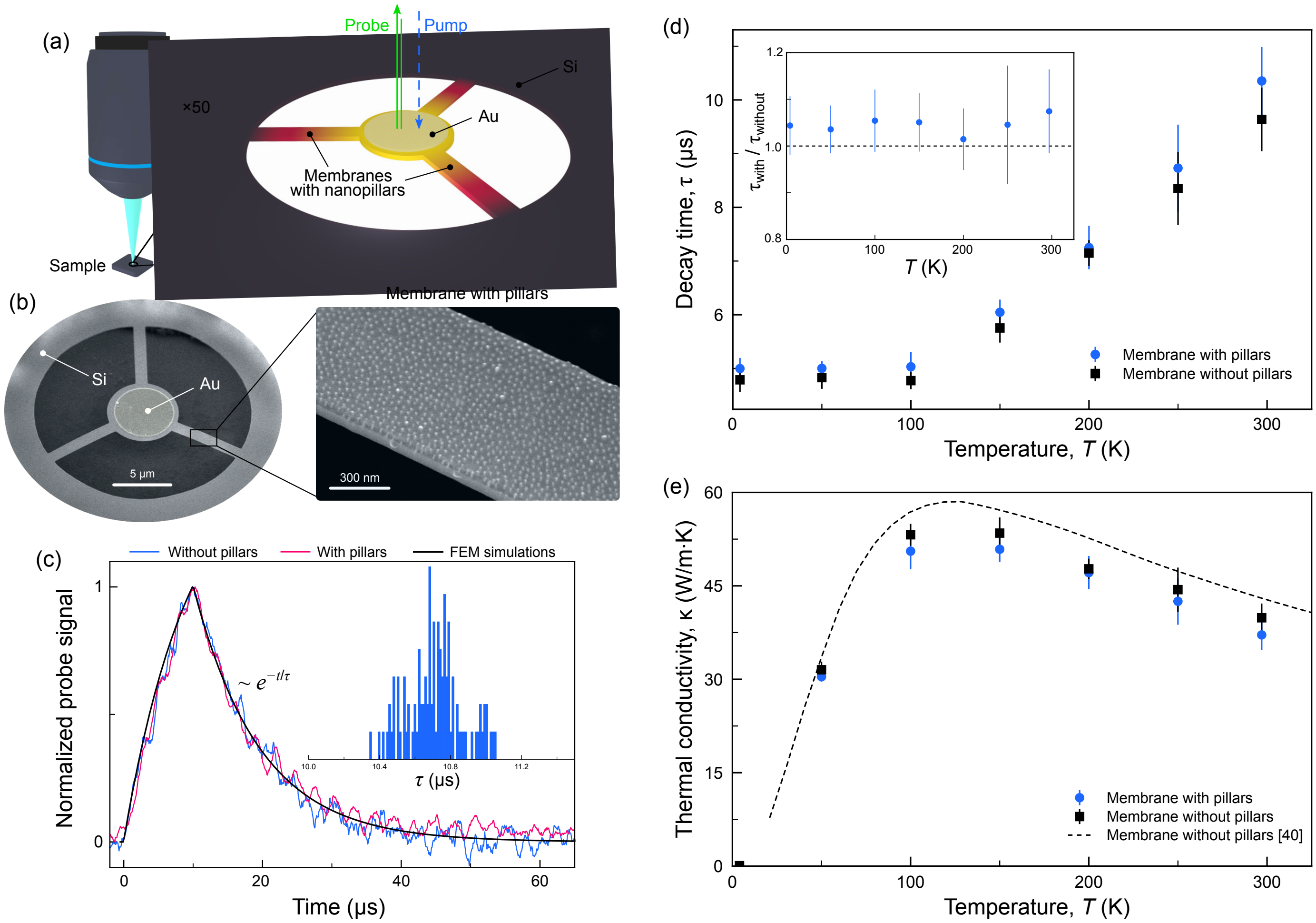

Fig. 3 (a) Scheme of the μTDTR experiment. (b) SEM images of a typical structure for the μTDTR experiment. (c) Example of probe beam signal with FEM model fit. Inset shows Gaussian statistical distribution of 100 measured decay times on one sample. (d) Thermal decay times through silicon membranes with and without nanopillars and (inset) their ratio showing no statistically significant difference. (e) Thermal conductivity of silicon membranes with and without nanopillars measured at different temperatures.

where the impact of low-frequencies resonant modes should be more substantial, we observed no statistically significant difference in the decay time, as shown in the inset of Fig. 3d. In other words, heat dissipation rate has not been noticeably affected by the presence of nanopillars.

Next, we converted the measured decay times into thermal conductivity. The conversion was performed using FEM simulations where the thermal conductivity of the membranes was used as a free parameter, as described in our previous work[39]. The obtained thermal conductivity also revealed no statistically significant difference between the values for membranes with and without nanopillars. Figure 3e shows that the thermal conductivity of membranes with nanopillars is only a few percent lower than that of a membranes without nanopillars in the entire range of temperatures. Overall, the values are consistent with the theoretical predictions by Malhotra and Maldovan[40] over the 50 – 300 K range. Likewise, the values are consistent with our previous measurements on the 50-nm-thick membranes[27,29].

Summary and outlook

In this work, we fabricated nanopillars on the surface thin membrane and investigated their impact on the phonon and thermal properties of the membrane. First, we measured the phonon dispersion of the silicon surface covered with nanopillars and detected the first resonant mode at 5 GHz with zero group velocity. This result confirms the theoretical predictions that nanopillars host localized phonon modes. Yet, such low-frequency modes seem unlikely to affect the thermal properties at room temperatures as the phonon spectrum spans over the terahertz rage and might only play a role at temperatures around a few kelvin. Future experimental works should aim to probe the vibrational modes in nanopillars at higher frequencies. Indeed, although present and previous works struggled to detect modes above a few gigahertz[22–26], it is plausible that more sensitive experiments could observe vibrational frequencies at least in the tens of gigahertz range, as was demonstrated for larger nanowires[41].

Next, we compared the thermal conductivity of silicon membranes with and without nanopillars on the surface. These experiments showed that the nanopillars reduced the thermal conductivity by only about five percent, which is within the uncertainty range of our experiment. This result contrasts with the various theoretical predictions of the thermal conductivity reduction spanning from 40%[13,30] to two orders of magnitude depending on the size of nanopillars[16,19]. Specifically, pioneering simulations by Davis and Hussein[13] predicted 40% reduction in the thermal conductivity of the 50-nm-thick silicon membranes with 80-nm-tall pillars of 20 nm in diameter, which is very close to the nanopillars in our samples. However, most theoretical works simulate structures of atomic scale whereas the experimental samples remain at nanoscale and seem unlikely to reach atomic scale in foreseeable future. In this regard, future theoretical works should clarify the magnitude of reduction in thermal conductivity expected for the nanostructures of realistic size.

However, since the nanopillars have somewhat degraded after the preparation for the μTDTR experiments, the absence of the nanopillar impact on the heat conduction might also be attributed to the reduced size and quality of the nanopillars. Future experimental efforts should try to preserve the nanopillar quality during the fabrication process. Specifically, exposure to plasma and acids, required for the fabrication of suspended structures, tends to etch silicon nanopillars, especially if a native oxide was allowed to form on their surface. Any applications of nanopillars in microelectronic devices will require solving such fabrication issues, for instance by forming the nanopillars as a last fabrication step or creating a protective layer on the nanopillars.

Moreover, the density of our nanopillars on the surface is rather low while their positions are aperiodic, which could also explain their negligible coherent impact on thermal transport. Although the impact of local resonances is not expected to depend on the periodicity[14,42,43], simulations usually place nanopillars as a periodic array with a high density of nanopillars[13,16,19,30]. Future theoretical works should further clarify if the density and periodicity of nanopillars are important factors in predicted thermal conductivity reduction.

Acknowledgements

This work was supported by PRESTO JST (No. JPMJPR19I1), CREST JST (No. JPMJCR19Q3), and KAKENHI (No. 20H05649). We also thank Xin Huang, Sebastian Volz, and Bartlomiej Graczykowski for advice and discussions.

Author Contributions

R.A. fabricated the μTDTR samples, performed μTDTR and BLS measurements, analyzed the data, and prepared the article; D.O. fabricated the wafers with nanopillars; Y.W. contributed to the sample fabrication and BLS measurements; L.J. contributed to the μTDTR experiments; R.Y. contributed to sample fabrication; M.N. and S.S. contributed to the design of the study, project management, and funding acquisition; All authors contributed to the article preparation.

Conflicts of interest

The authors declare no conflicts of interest.

Notes and references

1 G. J. Snyder and E. S. Toberer, *Nature Materials*, 2008, **7**, 105–114.
2 T. Mori, *Small*, 2017, **13**, 1702013.
3 Q. Zhang, K. Deng, L. Wilkens, H. Reith and K. Nielsch, *Nature Electronics*, 2022, **5**, 333–347.
4 Y. Nakamura, *Science and Technology of Advanced Materials*, 2018, **19**, 31–43.
5 M. Haras, V. Lacatena, F. Morini, J.-F. Robillard, S. Monfray, T. Skotnicki and E. Dubois, *Materials Letters*, 2015, **157**, 193–196.
6 G. Schierning, *Physica Status Solidi A*, 2014, **211**, 1235–1249.
7 R. Yanagisawa, N. Tsujii, T. Mori, P. Ruther, O. Paul and M. Nomura, *Applied Physics Express*, 2020, **13**, 095001.
8 M. Nomura, R. Anufriev, Z. Zhang, J. Maire, Y. Guo, R. Yanagisawa and S. Volz, *Materials Today Physics*, 2022, **22**, 100613.
9 A. George, R. Yanagisawa, R. Anufriev, J. He, N. Yoshie, S. Volz and M. Nomura, *ACS Applied Materials & Interfaces*, 2019, **11**, 12027–12031.
10 S. Neogi, J. S. Reparaz, L. F. C. Pereira, B. Graczykowski, M. R. Wagner, M. Sledzinska, A. Shchepetov, M. Prunnila, J. Ahopelto, C. M. Sotomayor-Torres and D. Donadio, *ACS Nano*, 2015, **9**, 3820–3828.
11 S. Neogi and D. Donadio, *Physical Review Applied*, 2020, **14**, 024004.
12 S. Xiong, D. Selli, S. Neogi and D. Donadio, *Physical Review B*, 2017, **95**, 180301.
13 B. L. Davis and M. I. Hussein, *Physical Review Letters*, 2014, **112**, 055505.
14 R. Pourabolghasem, A. Khelif, S. Mohammadi, A. A. Eftekhar and A. Adibi, *Journal of Applied Physics*, 2014, **116**, 013514.
15 R. Anufriev and M. Nomura, *Nanomaterials*, 2019, **9**, 142.
16 Y. Jin, Y. Pennec, B. Bonello, H. Honarvar, L. Dobrzynski, B. Djafari-Rouhani and M. Hussein, *Reports on Progress in Physics*, 2021.
17 R. Anufriev and M. Nomura, *Physical Review B*, 2017, **95**, 155432.
18 D. Ma, A. Arora, S. Deng, J. Shiomi and N. Yang, *Materials Today Physics*, 2019, **8**, 56–61.
19 H. Honarvar and M. I. Hussein, *Physical Review B*, 2018, **97**, 195413.
20 H. Wang, Y. Cheng, Z. Fan, Y. Guo, Z. Zhang, M. Bescond, M. Nomura, T. Ala-Nissila, S. Volz and S. Xiong, *Nanoscale*, 2021, **13**, 10010–10015.
21 R. Anufriev and M. Nomura, *Science and Technology of Advanced Materials*, 2018, **19**, 863–870.
22 B. Graczykowski, M. Sledzinska, F. Alzina, J. Gomis-Bresco, J. S. Reparaz, M. R. Wagner and C. M. Sotomayor Torres, *Physical Review B*, 2015, **91**, 075414.
23 A. Trzaskowska, S. Mielcarek and J. Sarkar, *Journal of Applied Physics*, 2013, **114**, 134304.
24 D. Yudistira, A. Boes, B. Graczykowski, F. Alzina, L. Y. Yeo, C. M. Sotomayor Torres and A. Mitchell, *Physical Review B*, 2016, **94**, 094304.

25 A. Trzaskowska, P. Hakonen, M. Wiesner and S. Mielcarek, *Ultrasonics*, 2020, **106**, 106146.

26 M. Sledzinska, B. Graczykowski, F. Alzina, J. Santiso Lopez and C. M. Sotomayor Torres, *Microelectronic Engineering*, 2016, **149**, 41–45.

27 X. Huang, S. Gluchko, R. Anufriev, S. Volz and M. Nomura, *ACS Applied Materials & Interfaces*, 2019, **11**, 34394–34398.

28 R. Anufriev, R. Yanagisawa and M. Nomura, *Nanoscale*, 2017, **9**, 15083–15088.

29 X. Huang, D. Ohori, R. Yanagisawa, R. Anufriev, S. Samukawa and M. Nomura, *ACS Applied Materials & Interfaces*, 2020, **12**, 25478–25483.

30 Z. Wei, J. Yang, K. Bi and Y. Chen, *Journal of Applied Physics*, 2015, **118**, 155103.

31 D. Ohori, M. Murata, A. Yamamoto, K. Endo, M.-H. Chuang, M.-Y. Lee, Y. Li, J.-H. Tarng, Y.-J. Lee and S. Samukawa, 2021 IEEE 21st International Conference on Nanotechnology (NANO), 2021, pp. 199–202.

32 M.-H. Chuang, D. Ohori, Y. Li, K.-R. Chou and S. Samukawa, *Vacuum*, 2020, **181**, 109577.

33 H. Honarvar, L. Yang and M. I. Hussein, *Applied Physics Letters*, 2016, **108**, 263101.

34 F. Kargar and A. A. Balandin, *Nature Photonics*, 2021, **15**, 720–731.

35 B. Graczykowski, A. Gueddida, B. Djafari-Rouhani, H.-J. Butt and G. Fytas, *Physical Review B*, 2019, **99**, 165431.

36 H. Honarvar and M. I. Hussein, *Physical Review B*, 2016, **93**, 081412.

37 R. Yanagisawa, J. Maire, A. Ramiere, R. Anufriev and M. Nomura, *Applied Physics Letters*, 2017, **110**, 133108.

38 R. Anufriev, S. Gluchko, S. Volz and M. Nomura, *ACS Nano*, 2018, **12**, 11928–11935.

39 R. Anufriev, Y. Wu, J. Ordonez-Miranda and M. Nomura, *NPG Asia Materials*, 2022, **14**, 35.

40 A. Malhotra and M. Maldovan, *Journal of Applied Physics*, 2016, **120**, 204305.

41 F. Kargar, B. Debnath, J.-P. P. Kakko, A. Saÿnätjoki, H. Lipsanen, D. L. Nika, R. K. Lake, A. A. Balandin, A. Säynätjoki, H. Lipsanen, D. L. Nika, R. K. Lake and A. A. Balandin, *Nature Communications*, 2016, **7**, 13400.

42 D. Ma, H. Ding, H. Meng, L. Feng, Y. Wu, J. Shiomi and N. Yang, *Physical Review B*, 2016, **94**, 165434.

43 Y. Achaoui, V. Laude, S. Benchabane and A. Khelif, *Journal of Applied Physics*, 2013, **114**, 104503.